Transaction A: Civil Engineering
Vol. 17, No. 6, pp. 415–429

SCIENTIA IRANICA

Effect of Hydrostatic Pressure on Vibrating Rectangular Plates Coupled with Fluid

K. Khorshidi[1]

Abstract. *This study is focused on the hydrostatic vibration analysis of a rectangular plate in partial contact with a bounded fluid in bottom and vertical directions. A set of admissible trial functions is required to satisfy the clamped and simply supported geometric boundary conditions. The fluid velocity potential satisfying fluid boundary conditions is derived, and the wet dynamic modal functions of the plate are expanded, in terms of the finite Fourier series, for a compatibility requirement along the contacting surface between the plate and the fluid. The natural frequencies of the plate coupled with sloshing fluid modes are calculated using the Rayleigh-Ritz method, based on minimizing the Rayleigh quotient. The proposed analytical method is verified by comparing the presented results with the results obtained by three-dimensional finite element analysis. Finally, the influence of boundary conditions, plate and tank dimensions, fluid depth and hydrostatic pressure on natural frequencies is examined and discussed in detail.*

Keywords: *Vibration; Rectangular plate; Sloshing fluid; Hydrostatic pressure; Mod shape.*

INTRODUCTION

During past decades, different approximate solutions have been presented by investigators to predict natural frequencies of structures contacting a fluid. There have been many theoretical and experimental studies devoted to vibration analysis of plates in contact with a static fluid. Fu and Price [1] studied the vibration response of cantilever plates partially or totally immersed within a fluid. They used a combination of the finite element method and a singularity distribution panel approach, and they examined the effects of free surface, immersed length and depth on the dynamic characteristics. Robinson and Palmer [2] performed a modal analysis of a rectangular plate floating on a body of fluid. They derived the transfer function for a harmonic point load, but the analysis is valid only for a finite number of lower frequency modes. Hosseini-Hashemi et al. [3] proposed an analytical-numerical solution for the free vibration of multi-span, moderately thick, rectangular plates. In their work, the resulting Galerkin equation was solved by application of the Rayleigh-Ritz minimization method. Civalek used the HDQ-FD [4], DQ and HDQ [5], and DSC-HDQ [6] methods to predict the nonlinear static and dynamic behavior of rectangular plates. Kwak [7] studied the free vibration of rectangular plates floating on unbounded fluids. In his numerical approach which was based on a piecewise division, beam functions were used as admissible functions for the Rayleigh-Ritz and Green function combined method. Haddara and Cao [8] derived an approximate expression of the modal added masses for cantilever rectangular plates horizontally submerged in fluid using experimental and analytical data. They also studied the effect of boundary conditions and submergence depth. Zhou and Cheung [9] investigated vibration characteristics of a rectangular plate in contact with fluid on one side employing the Rayleigh-Ritz approach. In their study, the fluid is filled in a rigid rectangular domain, which has a free surface and is infinite in the length direction. Similarly, Cheung and Zhou [10] studied natural frequencies of an elastic plate located in a rectangular hole and fixed to the rigid bottom slab of

1. *Sound and Vibration Laboratory, Department of Mechanical Engineering, Faculty of Engineering, Arak University, Arak, P.O. Box 38156-8-8349, Iran. E-mail: k-khorshidi@araku.ac.ir*

Received 4 August 2009; received in revised form 18 August 2010; accepted 19 October 2010

a fluid container. They employed the Ritz method for the analysis. Chang and Liu [11] calculated the natural frequencies of a rectangular isotropic plate in contact with fluid for various boundary conditions. They observed that the wet modes were almost identical to the dry mode shapes. Liang et al. [12] suggested a simple procedure to determine the natural frequencies and mode shapes of submerged cantilever plates, based on empirical added mass formulation. Yadykin et al. [13] estimated the added mass of a rectangular plate immersed in a fluid for the various aspect ratios. It was assumed that the plate is clamped at one edge and free at other edges, and the added mass is only calculated for a spanwise half-sine fundamental mode. An analytical method for the free vibration of a flexible rectangular plate [14] and two flexible rectangular plates [15,16] in contact with water is developed by the Rayleigh-Ritz method. Jeong et al. in [14-16] assumed that the wet displacement of each plate is a combination of the modal function of a dry uniform beam with a clamped boundary condition. They used the velocity potential of the fluid, satisfying the fluid boundary conditions using the finite Fourier series. Ergin and Uğurlu [17] investigated Cantilever plates partially submerged in a fluid, numerically, and studied the effect of plate aspect ratio. Recently, Zhou and Liu [18] developed a theory on the three-dimensional dynamic characteristics of flexible rectangular tanks partially filled with fluid, using a combination of the Rayleigh-Ritz and Galerkin methods. Uğurlu et al. [19] studied the dynamic behavior of rectangular plates mounted on an elastic foundation and in partial contact with a quiescent fluid. They employed a mixed-type finite element formulation to present the natural frequencies and associated mode shapes of the plate.

This paper presents a theory to calculate the natural frequencies of a rectangular plate partially contacting bounded fluid in the bottom and vertical direction, using the Rayleigh-Ritz method. In the developed model, the von Kármán linear strain-displacement relationships are used in order to obtain the kinetic and strain energies of the plate. The contributions given by the presence of the fluid and by the sloshing effects of the free surface are also included in the model. The system has then been studied in the case of a plate in contact with fluid on both sides. In this case, the contribution of the initial deformation of the plate, given by the hydrostatic pressure of the fluid, can be eliminated, if the fluid level in both tanks is identical. In conclusion, results show that fluid in contact with a plate on one or both sides completely changes the linear dynamics. Therefore, fluid-structure interaction must be carefully considered. The developed numerical models are able to reproduce such results with good accuracy.

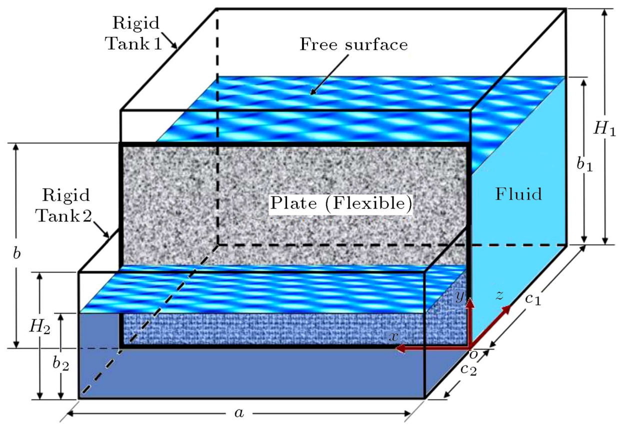

Figure 1. Geometry of the fluid-structure coupled system.

PLATE IN CONTACT WITH FLUID

Consider a rectangular thin plate with length a, width b, thickness h, and mass density ρ_p, which is part of the vertical side of two rigid tanks filled with fluid, as shown in Figure 1. The fluid in Tank 1, with depth b_1 (depth of the tank H_1), length a, width c_1 and mass density ρ_{F_1}, and in Tank 2, with depth b_2 (depth of the tank H_2), length a, width c_2 and mass density ρ_{F_2} are considered to be incompressible, inviscid and irrotational.

Formulation of Plate Oscillations

A rectangular plate with coordinates system $(Oxyz)$, having the origin O at one corner, is considered (see Figure 1). The displacements of an arbitrary point of coordinates $(x,\ y)$ on the middle surface of the plate are denoted by u, v and w, in the x, y and out-of-plane (z) directions, respectively. The von Kármán linear strain-displacement relationships are used. Strain components ε_x, ε_y and γ_{xy} at an arbitrary point of the plate are related to the middle surface strains, $\varepsilon_{x,0}$, $\varepsilon_{y,0}$ and $\gamma_{xy,0}$, and to the changes in the curvature and torsion of the middle surface, k_x, k_y and k_{xy}, by the following three relationships:

$$\varepsilon_x = \varepsilon_{x,0} + zk_x, \tag{1a}$$

$$\varepsilon_y = \varepsilon_{y,0} + zk_y, \tag{1b}$$

$$\gamma_{xy} = \gamma_{xy,0} + zk_{xy}, \tag{1c}$$

where z is the distance of the arbitrary point of the plate from the middle surface. According to von Kármán's theory, the middle surface strain-displacement relationships and changes in the curvature and torsion in absence of in-plane displacements are given by:

$$\varepsilon_{x,0} = \frac{\partial w}{\partial x}\frac{\partial w_0}{\partial x}, \tag{2}$$

$$\varepsilon_{y,0} = \frac{\partial w}{\partial y}\frac{\partial w_0}{\partial y}, \tag{3}$$

$$\gamma_{xy,0} = \frac{\partial w}{\partial x}\frac{\partial w_0}{\partial y} + \frac{\partial w_0}{\partial x}\frac{\partial w}{\partial y}, \tag{4}$$

$$k_x = -\frac{\partial^2 w}{\partial x^2}, \tag{5}$$

$$k_y = -\frac{\partial^2 w}{\partial y^2}, \tag{6}$$

$$k_{xy} = -2\frac{\partial^2 w}{\partial x \partial y}, \tag{7}$$

where w_0 is the out-of-plane displacement representing the initial geometric deformations of the plate associated with initial hydrostatic triangular pressure tension (see the Appendix for details). As a consequence, only isotropic and symmetric plates will be analyzed; there is no coupling between in-plane stretching and transverse bending. The elastic strain energy, U_P, of a plate, neglecting σ_z under Kirchhoff's hypotheses, is given by:

$$U_P = \frac{1}{2}\int_0^a\int_0^b\int_{-h/2}^{h/2} (\sigma_x\varepsilon_x + \sigma_y\varepsilon_y + \tau_{xy}\gamma_{xy})\, dzdydx. \tag{8}$$

For homogeneous and isotropic materials ($\sigma_z = 0$, case of plane stress), stress components σ_x, σ_y and τ_{xy} are related to the strain components as follows:

$$\sigma_x = \frac{E}{1-\nu^2}(\varepsilon_x + \nu\varepsilon_y), \tag{9a}$$

$$\sigma_y = \frac{E}{1-\nu^2}(\varepsilon_y + \nu\varepsilon_x), \tag{9b}$$

$$\tau_{xy} = \frac{E}{2(1+\nu)}\gamma_{xy}, \tag{9c}$$

where E is Young's modulus and ν is Poisson's ratio. Using Equations 1 to 9, the following expression is obtained:

$$U_P = \frac{1}{2}\frac{E}{1-\nu^2}\int_0^a\int_0^b\Bigg(\varepsilon_{x,0}^2 + \varepsilon_{y,0}^2 + 2\nu\varepsilon_{x,0}\varepsilon_{y,0} + \frac{1-\nu}{2}\gamma_{xy,0}^2\Bigg)dydx$$

$$+\frac{1}{2}\frac{Eh^3}{12(1-\nu^2)}\int_0^a\int_0^b\Bigg(k_x^2 + k_y^2 + 2\nu k_x^2 k_y^2 + \frac{1-\nu}{2}k_{xy}^2\Bigg)dydx, \tag{10}$$

where the first term is the membrane (also referred to as stretching) energy and the second one is the bending energy. The kinetic energy, T_P, of a rectangular plate, by neglecting rotary inertia and in-plane displacements, is given by:

$$T_P = \frac{1}{2}\rho_P h\int_0^a\int_0^b (\dot{w}^2)\, dydx, \tag{11}$$

where in Equation 11, the overdot denotes a time derivative.

Formulation of Fluid Oscillations

Using the principle of superposition, the fluid (the fluid surrounded by a vertical flexible rectangular plate and rigid tank walls in bottom and vertical directions is assumed to be incompressible, inviscid and irrotational) velocity potential, ϕ_O, can be obtained as:

$$\phi_O = \phi_B + \phi_S, \tag{12}$$

where ϕ_B describes the velocity potential of the fluid associated with plate bulging modes and ϕ_S is the velocity potential due to fluid sloshing (assuming the plate to be rigid). The fluid velocity potential, $\phi_O(x,y,z,t) = \varphi_O(x,y,z)\dot{T}(t)$, satisfies the Laplace equation in the fluid domain as follows:

$$\nabla^2\phi_O = \frac{\partial^2\phi_O}{\partial x^2} + \frac{\partial^2\phi_O}{\partial y^2} + \frac{\partial^2\phi_O}{\partial z^2}$$

$$= \nabla^2\phi_B + \nabla^2\phi_S = 0$$

$$\Rightarrow \nabla^2\phi_B = 0, \qquad \nabla^2\phi_S = 0, \tag{13}$$

where $\dot{T}(t) = dT(t)/dt$, and $\varphi_O(x,y,z)$ is deformation potential. Applying the method of separation of variables:

$$\phi_B(x,y,z,t) = \phi_B(x)\phi_B(y)\phi_B(z)\dot{T}(t),$$

to Equation 13, the following three uncoupled, second-order, ordinary differential equations are obtained:

$$\frac{1}{\phi_B(x)}\frac{d^2\phi_B(x)}{dx^2} + \frac{1}{\phi_B(y)}\frac{d^2\phi_B(y)}{dy^2} + \frac{1}{\phi_B(z)}\frac{d^2\phi_B(z)}{dz^2} = 0, \tag{14}$$

where the obtained ordinary differential equations can be written as:

$$\frac{1}{\phi_B(x)}\frac{d^2\phi_B(x)}{dx^2}=\pm p_1^2, \tag{15}$$

$$\frac{1}{\phi_B(y)}\frac{d^2\phi_B(y)}{dy^2}=\pm q_1^2, \tag{16}$$

$$\frac{1}{\phi_B(z)}\frac{d^2\phi_B(z)}{dz^2}=\mp(p_1^2+q_1^2), \tag{17}$$

where p_1^2 and q_1^2 are arbitrary nonnegative numbers. The boundary conditions on the horizontal and vertical sides of the Tank 1 (without sloshing) are expressed by:

For rigid walls boundary conditions:

$$\left.\frac{\partial\phi_{B1}}{\partial x}\right|_{x=0,a}=0, \tag{18}$$

$$\left.\frac{\partial\phi_{B1}}{\partial y}\right|_{y=0}=0, \tag{19}$$

$$\left.\frac{\partial\phi_{B1}}{\partial z}\right|_{z=c_1}=0. \tag{20}$$

For free surface (without sloshing) boundary conditions:

$$\left.\frac{\partial\phi_{B1}}{\partial t}\right|_{y=b_1}=\left.\phi_{B1}\right|_{y=b_1}=0. \tag{21}$$

For elastic wall boundary conditions:

$$\left.\frac{\partial\phi_{B1}}{\partial z}\right|_{z=o}=\frac{\partial w(x,y,t)}{\partial t}, \tag{22}$$

and the boundary conditions on the horizontal and vertical sides of Tank 2 (without sloshing) are expressed by:

For rigid walls boundary conditions:

$$\left.\frac{\partial\phi_{B2}}{\partial x}\right|_{x=0,a}=0, \tag{23}$$

$$\left.\frac{\partial\phi_{B2}}{\partial y}\right|_{y=0}=0, \tag{24}$$

$$\left.\frac{\partial\phi_{B2}}{\partial z}\right|_{z=-c_2}=0. \tag{25}$$

For free surface (without sloshing) boundary conditions:

$$\left.\frac{\partial\phi_{B2}}{\partial t}\right|_{y=b_2}=\left.\phi_{B2}\right|_{y=b_2}=0. \tag{26}$$

For elastic wall boundary conditions:

$$\left.\frac{\partial\phi_{B2}}{\partial z}\right|_{z=o}=\frac{\partial w(x,y,t)}{\partial t}, \tag{27}$$

where $w(x,y,t)$ is the transverse deflection of the plate. General solutions of Equations 15 to 17, from knowledge of ordinary differential equations, may easily be given as:

$$\phi_B(x)=a_1\sin(p_1x)+a_2\cos(p_1x), \tag{28}$$

$$\phi_B(y)=a_3\sin(q_1y)+a_4\cos(q_1y), \tag{29}$$

$$\phi_B(z)=a_5e^{\sqrt{p_1^2+q_1^2}z}+a_6e^{-\sqrt{p_1^2+q_1^2}z}. \tag{30}$$

Ignoring the sloshing effect for Tank 1 and substituting the boundary Conditions 18 to 21 in Equations 28 to 30, the following solution is obtained for fluid velocity potential:

$$\phi_{B1}(x,y,z,t)=\sum_{l_1=0}^{\infty}\sum_{k_1=0}^{\infty}A_{l_1,k_1}(t)\cos\left(\frac{l_1\pi x}{a}\right)$$
$$\cos\left(\frac{(2k_1+1)\pi y}{2b_1}\right)\left(e^{S_1z}+e^{S_1(2c_1-z)}\right),$$
$$(l_1,k_1=0,1,2,\cdots),\qquad(0\le x\le a),$$
$$(0\le y\le b_1),\qquad(0\le z\le c_1), \tag{31}$$

where $A_{l_1,k_1}(t)$ is the unknown constant and

$S_1=\pi\sqrt{\left(\frac{l_1}{a}\right)^2+\left(\frac{2k_1+1}{2b_1}\right)^2}$.

Applying Condition 22, one obtains:

$$\left.\frac{\partial\phi_{B1}(x,y,z,t)}{\partial z}\right|_{z=0}=\sum_{l_1=0}^{\infty}\sum_{k_1=0}^{\infty}A_{l_1,k_1}(t)$$
$$S_1(1-e^{2c_1S_1})\cos\left(\frac{l_1\pi x}{a}\right)$$
$$\cos\left(\frac{(2k_1+1)\pi y}{2b_1}\right)=\dot{W}(x,y,t). \tag{32}$$

The associated Fourier coefficients, $A_{l_1,k_1}(t)$, can be determined in the usual manner from those of the right-hand side of Equation 32:

$$A_{l_1,k_1}(t)=$$
$$\frac{\frac{\text{coff}_1}{ab_1}\int_0^a\int_0^{b_1}\left(\dot{w}(x,y,t)\cos\left(\frac{l_1\pi x}{a}\right)\cos\left(\frac{(2k_1+1)\pi y}{2b_1}\right)\right)dydx}{S_1\left(1-e^{2c_1S_1}\right)},$$

$$\text{coff}_1=\begin{cases}1 & \text{if}\quad l_1=k_1=0\\ 2 & \text{if}\quad l_1\text{ or }k_1=0\\ 4 & \text{if}\quad l_1\text{ and }k_1\neq 0\end{cases} \tag{33}$$

In a similar way, considering boundary Conditions 23 to 26 for Tank 2 and neglecting sloshing effects, one can drive the solution of the fluid velocity potential as follows:

$$\phi_{B2}(x,y,z,t)=\sum_{l_2=0}^{\infty}\sum_{k_2=0}^{\infty}A_{l_2,k_2}(t)\cos\left(\frac{l_2\pi x}{a}\right)$$

$$\cos\left(\frac{(2k_2+1)\pi y}{2b_2}\right)\left(e^{S_2 z}+e^{-S_2(2c_2+z)}\right),$$

$$(l_2,k_2=0,1,2,\cdots),\qquad (0\le x\le a),$$

$$(0\le y\le b_2),\qquad (-c_2\le z\le 0),\tag{34}$$

where:

$$S_2=\pi\sqrt{\left(\frac{l_2}{a}\right)^2+\left(\frac{2k_2+1}{2b_2}\right)^2},$$

and A_{l_2,k_2} is the unknown constant. Applying Condition 27, one obtains:

$$\left.\frac{\partial\phi_{B2}(x,y,z,t)}{\partial z}\right|_{z=0}=\sum_{l_2=0}^{\infty}\sum_{k_2=0}^{\infty}A_{l_2,k_2}(t)$$

$$S_2(1-e^{2c_2S_2})\cos\left(\frac{l_2\pi x}{a}\right)$$

$$\cos\left(\frac{(2k_2+1)\pi y}{2b_2}\right)=\dot{W}(x,y,t).\tag{35}$$

The associated Fourier coefficients, A_{l_2,k_2}, can be determined from those of the right-hand side of Equation 35:

$$A_{l_2,k_2}(t)=$$

$$\frac{\frac{\mathrm{coff}_2}{ab_2}\int_0^a\int_0^{b_2}\left(\dot{w}(x,y,t)\cos\left(\frac{l_2\pi x}{a}\right)\cos\left(\frac{(2k_2+1)\pi y}{2b_2}\right)\right)dydx}{S_2\left(1-e^{2c_2S_2}\right)},$$

$$\mathrm{coff}_2=\begin{cases}1 & \text{if} \quad l_2=k_2=0\\ 2 & \text{if} \quad l_2 \text{ or } k_2=0\\ 4 & \text{if} \quad l_2 \text{ and } k_2\neq 0\end{cases}\tag{36}$$

Applying the method of separation of variables, $\phi_S(x,y,z,t)=\phi_S(x)\phi_S(y)\phi_S(z)\dot{T}(t)$, to Equation 12, the following three uncoupled, second-order, ordinary differential equations are obtained:

$$\frac{1}{\phi_S(x)}\frac{d^2\phi_S(x)}{dx^2}+\frac{1}{\phi_S(y)}\frac{d^2\phi_S(y)}{dy^2}$$

$$+\frac{1}{\phi_S(z)}\frac{d^2\phi_S(z)}{dz^2}=0,\tag{37}$$

where the ordinary differential equations can be written as:

$$\frac{1}{\phi_S(x)}\frac{d^2\phi_S(x)}{dx^2}=\pm p_2^2,\tag{38}$$

$$\frac{1}{\phi_S(y)}\frac{d^2\phi_S(y)}{dy^2}=\mp(p_2^2+q_2^2),\tag{39}$$

$$\frac{1}{\phi_S(z)}\frac{d^2\phi_S(z)}{dz^2}=\pm q_2^2,\tag{40}$$

where p_2^2 and q_2^2 are arbitrary nonnegative numbers. The boundary conditions on the horizontal and vertical sides of Tank 1 without a flexible plate are expressed by:

For rigid walls:

$$\left.\frac{\partial\phi_{S1}}{\partial x}\right|_{x=0,a}=0,\tag{41}$$

$$\left.\frac{\partial\phi_{S1}}{\partial y}\right|_{y=0}=0,\tag{42}$$

$$\left.\frac{\partial\phi_{S1}}{\partial z}\right|_{z=0,c}=0,\tag{43}$$

and the sloshing boundary conditions on the horizontal and vertical sides of Tank 2 are expressed by:

For rigid walls:

$$\left.\frac{\partial\phi_{S2}}{\partial x}\right|_{x=0,a}=0,\tag{44}$$

$$\left.\frac{\partial\phi_{S2}}{\partial y}\right|_{y=0}=0,\tag{45}$$

$$\left.\frac{\partial\phi_{S2}}{\partial z}\right|_{z=0,-c_2}=0.\tag{46}$$

The general solutions of Equations 38 to 40, from knowledge of ordinary differential equations, may easily be given as:

$$\phi_S(x)=a_7\sin(p_2x)+a_8\cos(p_2x),\tag{47}$$

$$\phi_S(y)=a_9e^{\sqrt{p_2^2+q_2^2}y}+a_{10}e^{-\sqrt{p_2^2+q_2^2}y},\tag{48}$$

$$\phi_S(z)=a_{11}\sin(q_2z)+a_{12}\cos(q_2z).\tag{49}$$

Considering the boundary Conditions 41 to 43 and Equations 47 to 49, one obtains the solutions of the sloshing velocity potential of the fluid in Tank 1 as follows:

$$\phi_{S1}(x,y,z,t)=\sum_{i_1=0}^{\infty}\sum_{j_1=0}^{\infty}B_{i_1,j_1}(t)\cos\left(\frac{i_1\pi x}{a}\right)\cosh(S_3 y)\cos\left(\frac{j_1\pi z}{c_1}\right),$$

$$(i_1,j_1=0,1,2,\cdots),\qquad (0\le x\le a),$$

$$(0\le y\le b_1),\qquad (0\le z\le c_1). \tag{50}$$

where:

$$S_3=\pi\sqrt{\left(\frac{i_1}{a}\right)^2+\left(\frac{j_1}{c_1}\right)^2},$$

and $B_{i_1,j_1}(t)$ is the unknown constant.

Considering the boundary Conditions 44 to 46 and Equations 47 to 49, one obtains the solutions of the velocity potential of the sloshing fluid for Tank 2 as follows:

$$\phi_{S2}(x,y,z,t)=\sum_{i_2=0}^{\infty}\sum_{j_2=0}^{\infty}B_{i_2,j_2}(t)\cos\left(\frac{i_2\pi x}{a}\right)\cosh(S_4 y)\cos\left(\frac{j_2\pi z}{c_1}\right),$$

$$(i_2,j_2=0,1,2,\cdots),\qquad (0\le x\le a),$$

$$(0\le y\le b_2),\qquad (-c_2\le z\le 0), \tag{51}$$

where:

$$S_4=\pi\sqrt{\left(\frac{i_2}{a}\right)^2+\left(\frac{j_2}{c_2}\right)^2},$$

and $B_{i_2,j_2}(t)$ is the unknown constant.

Employing the hypothesis of incompressible, inviscid, irrotational fluid and no surface waves, the kinetic energy of the fluid with respect to the bulging modes of the plate (T_{fB_1} with respect to Tank 1, and T_{fB_2} with respect to Tank 2), can be expressed as follows:

$$T_{fB1}=\frac{1}{2}\rho_{F_1}\int_0^a\int_0^{b_1}\phi_{B1}|_{z=0}\left(-\frac{\partial w}{\partial t}\right)dydx, \tag{52}$$

$$T_{fB2}=\frac{1}{2}\rho_{F_2}\int_0^a\int_0^{b_2}\phi_{B2}|_{z=0}\left(\frac{\partial w}{\partial t}\right)dydx. \tag{53}$$

The kinetic energy terms corresponding to the fluid sloshing (with surface waves) in Tanks 1 and 2 are expressed as follows:

$$T_{fS1}=\frac{1}{2}\rho_{F_1}\int_0^a\int_0^{b_1}\phi_{S1}|_{z=0}\left(-\frac{\partial w}{\partial t}\right)dydx, \tag{54}$$

$$T_{fS2}=\frac{1}{2}\rho_{F_2}\int_0^a\int_0^{b_2}\phi_{S2}|_{z=0}\left(\frac{\partial w}{\partial t}\right)dydx. \tag{55}$$

The linearized sloshing conditions at the fluid free surface of Tank 1 and Tank 2 are [20]:

$$\left.\frac{\partial\phi_{O1}}{\partial y}\right|_{y=b_1}=\frac{\omega^2}{g}\phi_{O1}\Big|_{y=b_1}, \tag{56}$$

$$\left.\frac{\partial\phi_{O2}}{\partial y}\right|_{y=b_2}=\frac{\omega^2}{g}\phi_{O2}\Big|_{y=b_2}, \tag{57}$$

where g is the gravity acceleration, ϕ_{O1} is the velocity potential of fluid in Tank 1, ϕ_{O2} is the velocity potential of fluid in Tank 2 and ω is the circular frequency of the plate and sloshing fluid. Substituting Equation 12 into Equations 56 and 57, and using Equations 21 and 26, one obtains:

$$\left.\frac{\partial\phi_{B1}}{\partial y}\right|_{y=b_1}+\left.\frac{\partial\phi_{S1}}{\partial y}\right|_{y=b_1}=\frac{\omega^2}{g}\phi_{S1}\Big|_{y=b_1}, \tag{58a}$$

$$\left.\frac{\partial\phi_{B2}}{\partial y}\right|_{y=b_2}+\left.\frac{\partial\phi_{S2}}{\partial y}\right|_{y=b_2}=\frac{\omega^2}{g}\phi_{S2}\Big|_{y=b_2}. \tag{58b}$$

Multiplying both sides of Equation 58a by $\rho_{F_1}\phi_{S1}$, then integrating them over the free surface of the fluid in Tank 1, and in a similar way, multiplying both sides of Equation 58b by $\rho_{F_2}\phi_{S2}$, then integrating them over the free surface of the fluid in Tank 2, one can obtain:

$$U_{\phi_{B1}}+U_{\phi_{S1}}=\omega^2T_{\phi_{S1}}, \tag{59a}$$

$$U_{\phi_{B2}}+U_{\phi_{S2}}=\omega^2T_{\phi_{S2}}, \tag{59b}$$

where:

$$U_{\phi_{B1}}=\rho_{F_1}\int_0^a\int_0^{c_1}\left(\phi_{S1}\frac{\partial\phi_{B1}}{\partial y}\right)_{y=b_1}dzdx, \tag{60}$$

$$U_{\phi_{S1}}=\rho_{F_1}\int_0^a\int_0^{c_1}\left(\phi_{S1}\frac{\partial\phi_{S1}}{\partial y}\right)_{y=b_1}dzdx, \tag{61}$$

$$T_{\phi S1} = \frac{\rho_{F_1}}{g} \int_0^a \int_0^{c_1} (\phi_{S1}^2)_{y=b_1} dz dx, \tag{62}$$

$$U_{\phi B2} = \rho_{F_2} \int_0^a \int_{-c_2}^0 \left(\phi_{S2} \frac{\partial \phi_{B2}}{\partial y} \right)_{y=b_2} dz dx, \tag{63}$$

$$U_{\phi S2} = \rho_{F_2} \int_0^a \int_{-c_2}^0 \left(\phi_{S2} \frac{\partial \phi_{S2}}{\partial y} \right)_{y=b_2} dz dx, \tag{64}$$

$$T_{\phi S2} = \frac{\rho_{F_2}}{g} \int_0^a \int_{-c_2}^0 (\phi_{S2}^2)_{y=b_2} dz dx. \tag{65}$$

Rayleigh-Ritz Approach

The Lagrangian function of the fluid-plate system for free vibration is:

$$\Pi = \sum \text{Starin Energy}_{\max} - \sum \text{Kinetic Energy}_{\max}. \tag{66}$$

Using the Ritz finite series approximation method, and with the assumption of immovable simply supported and clamped boundary conditions, the components of the displacements field for the dry plate are estimated as follows:

$$w(x,y) = \sum_{m=1}^{M} \sum_{n=1}^{N} w_{m,n}(t) \sin(m\pi x/a) \sin(n\pi y/b), \tag{67}$$

where m and n are the numbers of half-waves in x and y directions, respectively, and t is the time and $w_{m,n}(t)$ are the generalized coordinates, which are unknown functions of t. M and N indicate the terms necessary in the expansion of out-of-plane displacement. The boundary conditions on bending moments for the clamped boundary condition of the plates can be approximated by assuming that rotational springs of very high stiffness, κ, are distributed along the plate edges, so additional potential energy, stored by elastic rotational springs at the plate edges, must be added. This potential energy, U_R, is given by [21]:

$$U_R = \frac{1}{2} \int_0^b \kappa \left\{ \left[\left(\frac{\partial w}{\partial x} \right)_{x=0} \right]^2 + \left[\left(\frac{\partial w}{\partial x} \right)_{x=a} \right]^2 \right\} dy$$
$$+ \frac{1}{2} \int_0^a \kappa \left\{ \left[\left(\frac{\partial w}{\partial y} \right)_{y=0} \right]^2 + \left[\left(\frac{\partial w}{\partial y} \right)_{y=b} \right]^2 \right\} dx. \tag{68}$$

In order to simulate clamped edges in numerical calculations, a very high value of stiffness ($\kappa \to \infty$) must be assumed. This approach is usually referred to as the artificial spring method, which can be regarded as a variant of the classical penalty method. The values of the spring stiffness simulating a clamped plate can be obtained by studying the convergence of the natural frequencies of the linearized solution by increasing the value of κ. In fact, it was found that the natural frequencies of the system converge asymptotically with those of a clamped plate when κ becomes very large (in this study the non-uniform stiffness is assumed as $\kappa = 10^8$).

Considering the plate motions to be harmonic (i.e. $\ddot{T}(t) = -\omega^2 T(t)$) and with the application of the Ritz minimization method, an eigenvalue equation can be derived from Equation 66:

$$\frac{\partial \Pi}{\partial q} = 0, \tag{69}$$

where q is the vector of generalized coordinates and contains the unknown time variable coefficients of the admissible trial functions presented by Equations 50, 51 and 67 (i.e. $q = \{w_{m,n}, B_{i_1,j_1}, B_{i_2,j_2}\}^T$).

Following minimization Equation 69, the subsequent equation is obtained:

$$(K_p + K_R)C_{m,n} - \omega^2[(M_P + M_{fB1} + M_{fB2})C_{m,n}$$
$$+ M_{fS1}B_{i_1,j_1} + M_{fS2}B_{i_2,j_2}] = 0, \tag{70}$$

where:

$$C_{m,n} = \{w_{m,n}\}^T,$$

and:

$$K_p = \frac{\partial^2 U_p}{\partial q_i \partial q_j}, \tag{71}$$

$$K_R = \frac{\partial^2 U_R}{\partial q_i \partial q_j}, \tag{72}$$

$$M_p = \frac{\partial^2 T_p}{\partial q_i \partial q_j}, \tag{73}$$

$$M_{fB1} = \frac{\partial^2 T_{fB1}}{\partial q_i \partial q_j}, \tag{74}$$

$$M_{fS1} = \frac{\partial^2 T_{fS1}}{\partial q_i \partial q_j}, \tag{75}$$

$$M_{fB2} = \frac{\partial^2 T_{fB2}}{\partial q_i \partial q_j}, \tag{76}$$

$$M_{fS2} = \frac{\partial^2 T_{fS2}}{\partial q_i \partial q_j}. \tag{77}$$

Equation 70 cannot be solved until expressions for B_{i_1,j_1} and B_{i_2,j_2} are unknown. Thus, Equations 59a and 59b are added to the Galerkin equation (Equation 70). This increases the dimensions of the associated eigenvalue problem from $(\bar{N} \times \bar{N})$ to $((\bar{N} + \tilde{N}) \times (\bar{N} + \tilde{N}))$, where $\bar{N}$ is the dimension of the coordinates vector $\{w_{m,n}\}^T$ and $\tilde{N}$ is the dimension of the coordinates vector $\{B_{i_1,j_1}, B_{i_2,j_2}\}^T$. Consequently, the following Galerkin equation is obtained [20]:

$$\begin{bmatrix} K_p + K_R & 0 & 0 \\ K_{\phi B1} & K_{\phi S1} & 0 \\ K_{\phi B2} & 0 & K_{\phi S2} \end{bmatrix} \begin{Bmatrix} C_{m,n} \\ B_{i_1,j_1} \\ B_{i_2,j_2} \end{Bmatrix}$$

$$-\omega^2 \begin{bmatrix} M_P + M_{fB1} + M_{fB2} & M_{fS1} & M_{fS2} \\ 0 & M_{\phi S1} & 0 \\ 0 & 0 & M_{\phi S2} \end{bmatrix}$$

$$\begin{Bmatrix} C_{m,n} \\ B_{i_1,j_1} \\ B_{i_2,j_2} \end{Bmatrix} = 0, \tag{78}$$

where:

$$K_{\phi B1} = \frac{\partial^2 U_{\phi B_1}}{\partial q_i \partial q_j}, \tag{79}$$

$$K_{\phi S1} = \frac{\partial^2 U_{\phi S_1}}{\partial q_i \partial q_j}, \tag{80}$$

$$M_{\phi S1} = \frac{\partial^2 T_{\phi S_1}}{\partial q_i \partial q_j}, \tag{81}$$

$$K_{\phi B2} = \frac{\partial^2 U_{\phi B2}}{\partial q_i \partial q_j}, \tag{82}$$

$$K_{\phi S2} = \frac{\partial^2 U_{\phi S2}}{\partial q_i \partial q_j}, \tag{83}$$

$$M_{\phi S2} = \frac{\partial^2 T_{\phi S2}}{\partial q_i \partial q_j}. \tag{84}$$

The circular frequency, ω, is obtained by solving the generalized eigenvalue problem defined by Equation 78.

EXAMPLE AND DISCUSSION

On the basis of the preceding analysis and in order to find the natural frequencies of a rectangular plate in air or in contact with the bounded fluid by the rigid container walls, the eigenvalue Equation 78 is calculated using Mathematica v.5 analytical software. In the present study, the frequency equation derived in the preceding sections involves an infinite series of algebraic terms. For convenience, the approximation series in different directions are taken of the same order ($N = M = 9$) and the numbers of admissible functions of the fluids are set as $N1 = M1 = N2 = M2 = 5$. Herein all results are presented for rectangular aluminum plates where Young's modulus $E = 69$ Gpa, material density $\rho_P = 2700$ kg/m^3, Poisson's ratio $\nu = 0.3$, $a = 0.36$ m, $b = 0.48$ m and thickness $h = 0.003$ m. The mechanical and geometrical properties of the fluid are:

$$c_1 = 0.2 \text{ m}, \qquad c_2 = 0.2 \text{ m},$$

$$\rho_{F1} = 1000 \text{ kg/m}^3, \qquad \rho_{F2} = 1000 \text{ kg/m}^3.$$

Effect of Hydrostatic Pressure on Natural Frequency

The typical initial geometric deformations of the plate due to the hydrostatic pressure of the fluid on one side are illustrated in Figure 2. From this figure, it is observed that the initial geometric deformations of the plate due to hydrostatic pressure are distorted from the flat shapes of the dry rectangular plate. It is also observed that the initial geometric deformations change according to the fluid depth.

The effects of hydrostatic pressure on the natural frequency are shown in Figure 3. The results shown in Figure 3 were obtained for the steel, simply supported rectangular plate in contact with water. It is observed that between two plates with the same length, width, thickness and boundary conditions, the natural frequency of the plate with initial geometric deformations is bigger than the natural frequency of the plate without initial geometric deformations.

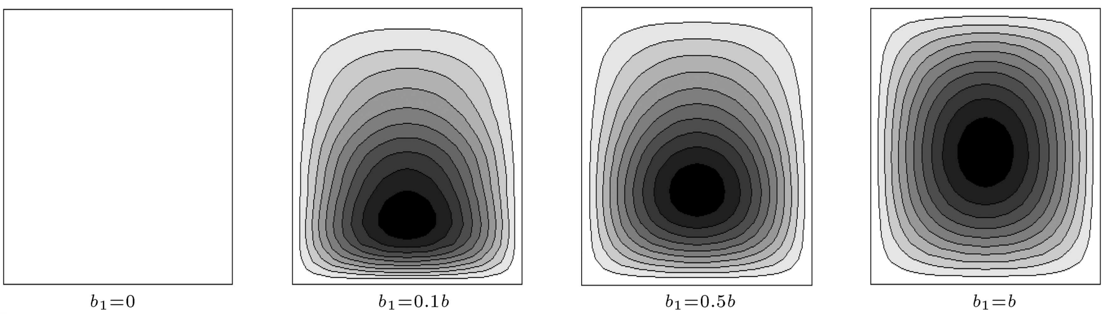

Figure 2. Typical static plate configuration due to hydrostatic triangular pressure for different fluid depth ratios.

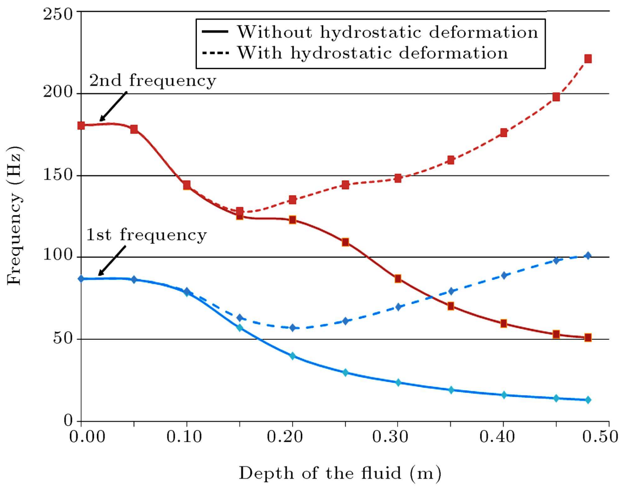

Figure 3. Variation of first fourth frequencies of S-S-S-S rectangular plate versus depth of the fluid (b_1) (case of plate in contact on one side with water).

Effect of Fluid Tank Dimension on Plate Mode Shape

Typical wet mode shapes are illustrated in Figures 4 and 5. The results given in these figures correspond to the case where Tank 1 is filled with water to half height and Tank 2 is empty. The effect of interaction between the plate and fluid causes the wet mode shapes to be distorted from the dry mode shapes of the rectangular plate. It is also observed that the mode shapes change according to the fluid depth. Especially, severely distorted shapes from dry mode shapes can be observed in higher modes. In higher wet modes, it is very difficult to categorize an equivalent dry mode due to the distortion of mode shape.

Effect of Fluid Depth on Natural Frequency

The wet natural frequencies of the rectangular plate in contact with fluid are always less than the corresponding natural frequency of the plate in air. Due to this fact, when normalizing the natural frequency, with respect to the free plate natural frequencies, one can see that defined normalized natural frequencies of a fluid-structure coupled system always lie between unity and zero, as shown in Figure 6. The calculated wet natural frequencies are presented in Table 1 for the simply supported rectangular plates partially in contact with water on both sides (for various fluids depth b_1 and $b_2 = 0.12$, 0.24, 0.36 and 0.48). From this table, it can be realized that the wet natural frequencies decrease as fluid depth increases.

Additionally, from Figure 6, one can observe that all wet natural frequencies of the clamped plate are higher than the corresponding ones of the simply supported plate. Meanwhile, from results presented in Figure 6, it can be observed that in both cases, variations of wet natural frequencies versus fluid depth have similar behavior for the first three natural frequencies.

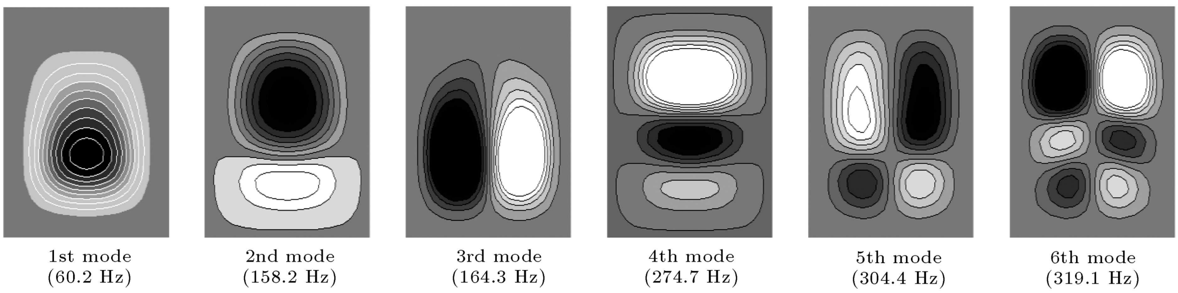

Figure 4. Typical mode shapes of a clamped rectangular plate partially contact with water for 50% fluid depth ratio (case of plate in contact on one side with water).

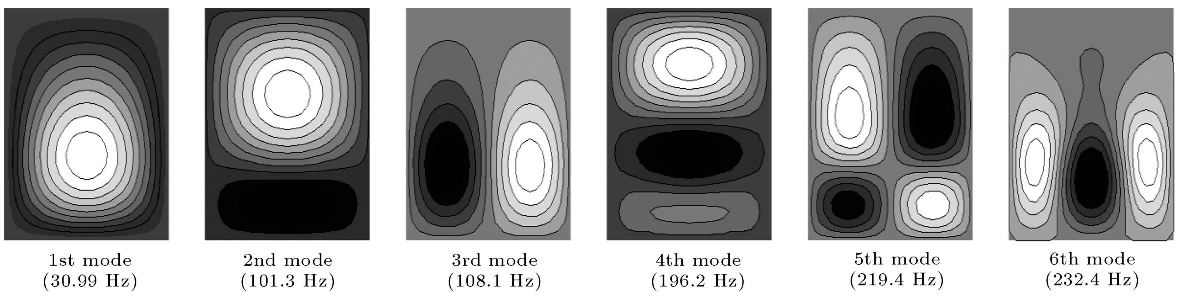

Figure 5. Typical mode shapes of a simply supported rectangular plate partially contact with water for 50% fluid depth ratio (case of plate in contact on one side with water).

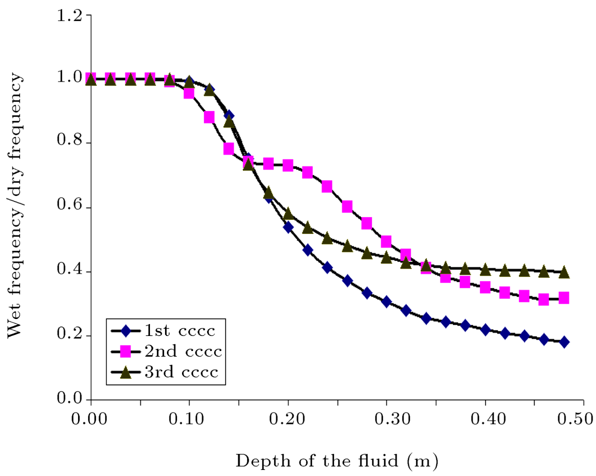

Rectangular plate with clamped B.Cs.
and dry frequencies;
$f_1 = 161.8$ Hz, $f_2 = 271.4$ Hz, $f_3 = 380.6$ Hz

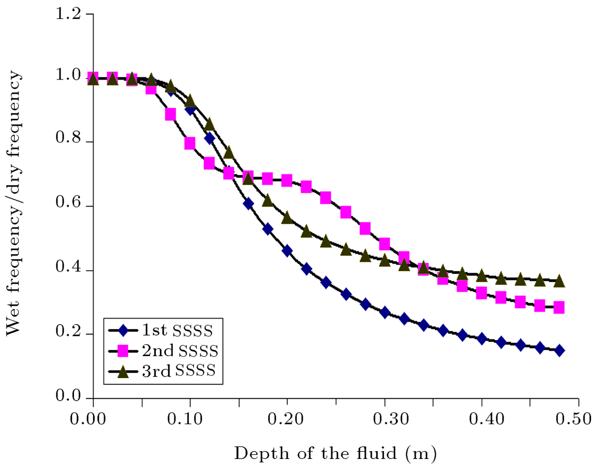

Rectangular plate with simply supported
B.Cs. and dry frequencies;
$f_1 = 86.91$ Hz, $f_2 = 180.78$ Hz, $f_3 = 253.79$ Hz

Figure 6. Variation of first three-dimensionless frequencies of rectangular plate versus depth of the fluid (b_1) (case of plate in contact on one side with water).

Effect of Fluid Tank Dimension on Natural Frequency

In order to study the effect of fluid tank dimensions on the plate wet natural frequencies, variations of three first dimensionless natural frequencies versus fluid tank dimension, c_1, have been plotted in Figure 7. In this figure, two plate boundary conditions are studied, i.e. simply supported and clamped boundary conditions. It is considered that the plate is partially in contact with water. The effect of tank dimensions, c_1 and c_2 (c_1 and c_2 = 0.1, 0.2 and 0.3), are also presented in Table 2. Figure 7 reveals that the wet natural frequency increases as the fluid tank dimension, c_1, increases.

Table 1. Variation of the natural frequencies of the wet rectangular plate with simply supported boundary conditions versus fluids depth ($c_1 = c_2 = 0.2$).

		Natural Frequency (Hz)			
b_1	b_2	f_1	f_2	f_3	f_4
0.12	0.12	58.531	122.465	170.437	267.081
	0.24	30.176	107.279	116.027	208.562
	0.36	18.249	64.205	98.645	144.075
	0.48	13.045	49.412	92.715	113.507
0.24	0.12	30.176	107.279	116.027	208.562
	0.24	22.871	92.452	95.613	195.750
	0.36	16.251	58.523	83.710	134.656
	0.48	12.308	44.285	82.093	105.883
0.36	0.12	18.249	64.205	98.645	144.075
	0.24	16.251	58.523	83.710	134.656
	0.36	13.206	49.751	74.022	115.944
	0.48	10.801	41.196	71.862	97.492
0.48	0.12	13.045	49.412	92.715	113.507
	0.24	12.308	44.285	82.093	105.883
	0.36	10.801	41.196	71.862	97.492
	0.48	9.329	36.966	68.373	87.856

Table 2. Variation of the natural frequencies of the wet rectangular plate with simply supported boundary conditions versus tanks dimension ($b_1 = 0.36$, $b_2 = 0.24$).

		Natural Frequency (Hz)			
c_1	c_2	f_1	f_2	f_3	f_4
0.1	0.1	13.023	54.546	78.246	130.115
	0.2	13.411	56.598	79.589	131.827
	0.3	13.491	57.070	79.714	132.010
0.2	0.1	15.573	56.268	82.166	132.787
	0.2	16.251	58.523	83.710	134.656
	0.3	16.394	59.063	83.853	134.858
0.3	0.1	16.515	56.382	82.680	132.935
	0.2	17.330	58.681	84.248	134.829
	0.3	17.504	59.242	84.393	135.033

Effect of Plate Dimensions on Natural Frequency

The effects of plate dimension, a, on plate wet natural frequencies for simply supported and clamped boundary conditions are graphically investigated in Figure 8. Inspection of curves given in Figure 8 gives an idea of how wet frequency varies when the length of plates increases, and width b, thickness h and boundary conditions remain identical. From this figure, one can see that the wet frequency decreases as plate dimension,

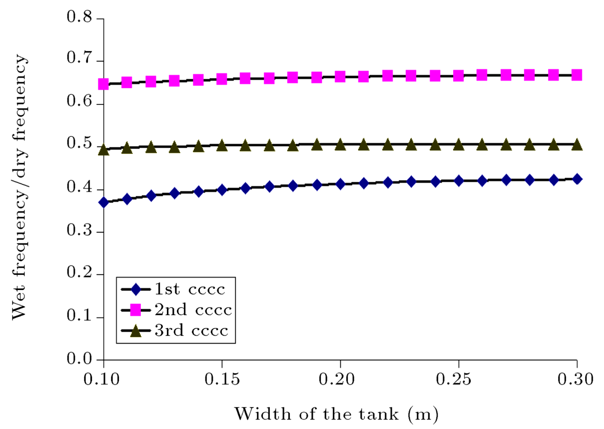

Rectangular plate with clamped B.Cs.
and dry frequencies;
$f_1 = 161.8$ Hz, $f_2 = 271.4$ Hz, $f_3 = 380.6$ Hz

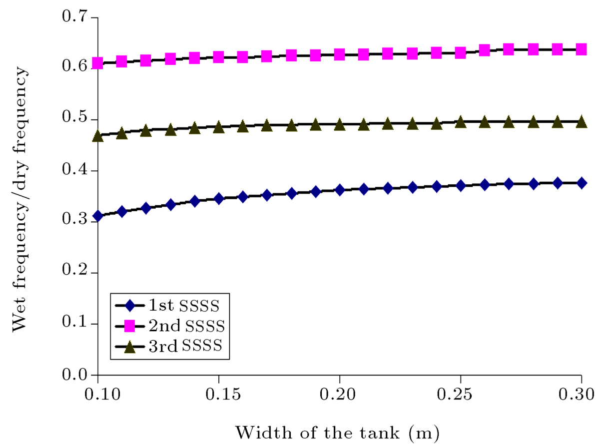

Rectangular plate with simply supported
B.Cs. and dry frequencies;
$f_1 = 86.91$ Hz, $f_2 = 180.78$ Hz, $f_3 = 253.79$ Hz

Figure 7. Variation of first three-dimensionless frequencies of rectangular plate versus width of the Tank 1 (c_1) (case of plate in contact on one side with water).

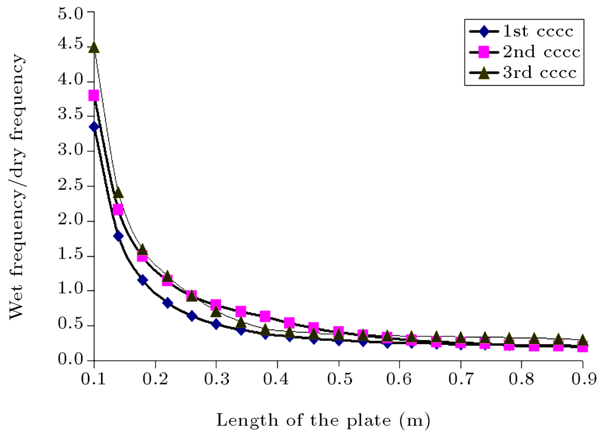

Rectangular plate with clamped B.Cs.
and dry frequencies;
$f_1 = 161.8$ Hz, $f_2 = 271.4$ Hz, $f_3 = 380.6$ Hz

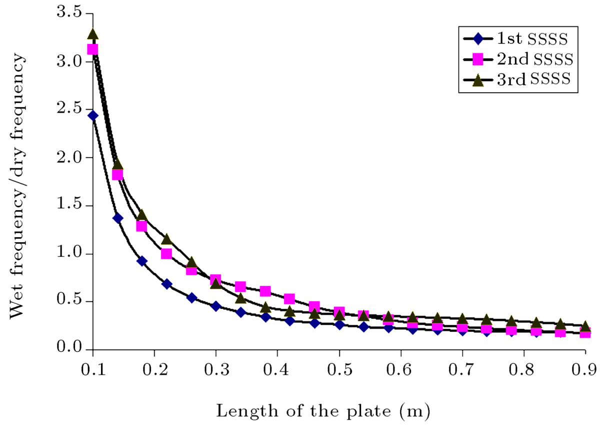

Rectangular plate with simply supported
B.Cs. and dry frequencies;
$f_1 = 86.91$ Hz, $f_2 = 180.78$ Hz, $f_3 = 253.79$ Hz

Figure 8. Variation of first three-dimensionless frequencies of rectangular plate versus length of the plate (a) (case of plate in contact on one side with water).

a, increases. Influences of the width of plates on the natural frequency are presented in Figure 9. The results shown in Figure 9 were obtained for the case of plate's both sides fluid-filled. It can be seen that with increasing the width of the plate, the natural frequency of the plate decreases.

Effect of Fluid Sloshing on Natural Frequency

In Table 3, the effects of fluid sloshing on the natural frequency of the plate are shown. For the same plate, fluid and size of tank, the natural frequency of the plate in contact with fluid with sloshing is lower than the natural frequency of the plate in contact with fluid without sloshing, because the effect of the kinetic energy of the fluid corresponding to the sloshing cause of frequency decreases in respect to fluid

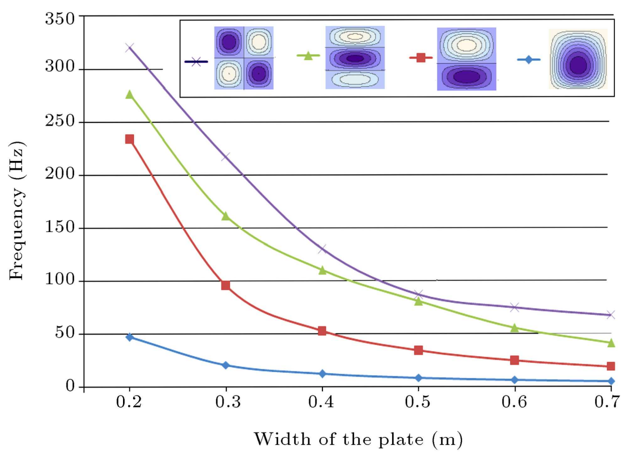

Figure 9. Variation of four frequencies of S-S-S-S rectangular plate versus width of the plate (b) (case of plate in contact on the both sides fluid-filled).

Table 3. The effect of fluid sloshing modes on first two wet natural frequency of the simply supported plate.

Depth of the Fluid in Tank 1 (m)	Natural Frequency (Hz)			
	With Sloshing		Without Sloshing	
	f_1	f_2	f_1	f_2
0	86.9136	180.78	86.9136	180.78
0.05	86.5522	177.922	86.5521	177.922
0.1	78.4684	143.845	78.4671	143.844
0.15	56.9888	125.587	56.9853	125.587
0.2	39.9908	122.71	39.9861	122.71
0.25	29.828	109.312	29.8226	109.312
0.3	23.4314	86.8349	23.4257	86.8337
0.35	19.1597	70.1461	19.1538	70.1448
0.4	16.1912	59.5525	16.1853	59.5513
0.45	14.0812	53.2317	14.0756	53.2309
0.48	13.1177	51.1994	13.1124	51.1988

without sloshing. But this effect is not taken into account.

COMPARISON WITH FINITE ELEMENT ANALYSIS

The modal results obtained, using the proposed theory, are compared with those of the finite element analysis to show the applicability, reliability and effectiveness of the presented formulation. The finite element analysis is carried out for the fluid-coupled system using a commercial computer code, ANSYS (release 9.0). For the Finite Element Method (FEM) analysis, the three-dimensional model is composed of three-dimensional contained fluid elements (FLUID80) and elastic shell elements (SHELL63). The results are shown in Table 4 for cases where Tank 1 is filled with water to half height and Tank 2 is empty. This table indicates that the present results are in excellent agreement with those of the finite element method.

CONCLUSION

An analytical method, based on the Rayleigh-Ritz method, for a rectangular plate partially contacting with a fluid, is developed. It is found that the normalized natural frequencies do not linearly decrease with fluid depth, tank dimension and plate dimension.

The main advantages of the analytical solutions presented in this paper can be summarized as follows.

Initial deformations due to hydrostatic triangular pressure have been taken into account, since they play a fundamental role. The initial deformations increase the rigidity of the plate and increase the natural frequency.

It has been also observed that fluid in contact with the plate on one or both sides changes the linear dynamics completely. Therefore, the fluid-structure interaction of the system must be carefully considered.

Table 4. Comparison of the natural frequencies of the dry and wet rectangular plate.

Serial Mode Number	Natural Frequency (Hz)							
	Simply Supported				Clamped			
	Dry		Wet (50%)		Dry		Wet (50%)	
	Present	ANSYS	Present	ANSYS	Present	ANSYS	Present	ANSYS
1	81.91	81.91	30.99	30.90	161.8	161.7	60.5	60.2
2	180.78	180.78	101.3	100.9	271.4	271.2	158.2	157.2
3	253.79	253.79	108.1	107.2	380.6	380.4	164.3	162.2
4	337.22	337.22	196.2	196.2	451.9	451.6	274.7	273.8
5	347.65	347.65	219.4	217.0	481.8	481.3	304.4	299.7
6	504.1	504.1	232.4	231.2	652.7	651.7	319.1	316.1
7	531.91	531.91	333.6	333.0	698.6	697.9	457.3	450.3
8	556.25	556.25	363.2	359.2	713.6	713	455.4	452.8
9	625.78	625.78	386.6	381.8	811.3	810.1	502.7	493.5
10	723.13	723.12	437.1	434.0	891.9	890.2	558.0	550.9

From the equation and results, it is observed that the contribution of the initial deformation of the plate, given by the hydrostatic pressure of the fluid, can be eliminated if the water level in both tanks is identical.

All results obtained by the present analytical solutions provide researchers and designers with a reliable source to validate the numerical results of their own problems.

NOMENCLATURE

a	length of the plate
b	width of the plate
h	thickness of the plate
ρ_p	mass density of the plate
E	Young's modulus of the plate
ν	Poisson's ratio of the plate
b_1	depth of the fluid in Tank 1
H_1	depth of the Tank 1
c_1	width of the Tank 1
ρ_{F_1}	mass density of the fluid in Tank 1
b_2	depth of the fluid in Tank 1
H_2	depth of Tank 1
c_2	width of Tank 1
ρ_{F_2}	mass density of the fluid in Tank 1
w	the transverse displacement of the plate
ε_x	normal strain in x-direction
ε_y	normal strain in y-direction
γ_{xy}	shear strain in xy-plane
σ_x	normal stress in x-direction
σ_u	normal stress in Y-direction
τ_{xy}	shear stress in xy-plane
U_p	the elastic strain energy of the plate
T_P	the kinetic energy of the plate
ϕ_O	total velocity potential of the fluid
ϕ_B	velocity potential of the fluid associated with plate bulging modes
ϕ_S	velocity potential due to fluid sloshing
φ_O	total deformation potential of the fluid
p_1^2, q_1^2 p_2^2 and q_2^2	arbitrary nonnegative numbers
T_{fB}	kinetic energy of the fluid with respect to the bulging modes
T_{fS}	kinetic energy terms corresponding to the fluid sloshing
g	gravity acceleration
Π	Lagrangian function
U_R	additional potential energy corresponding to clamped B.Cs.
κ	artificial elastic rotational springs coefficient
ω	natural frequency (rad/s)
f	natural frequency (Hz)

REFERENCES

1. Fu, Y. and Price, W.G. "Interactions between a partially or totally immersed vibrating cantilever plate and the surrounding fluid", *J. of Sound and Vibration*, **118**, pp. 495-513 (1987).

2. Robinson, N.J. and Palmer, S.C. "A modal analysis of a rectangular plate floating on an incompressible fluid", *J. of Sound and Vibration*, **142**, pp. 435-460 (1990).

3. Hosseini-Hashemi, Sh., Khorshidi, K. and Payandeh, H. "Vibration analysis of moderately thick rectangular plates with internal line support using Rayleigh-Ritz approach", *Scientia Iranica, Transaction B, Journal of Mechanical Engineering*, **16**(1), pp. 22-39 (2009).

4. Civalek, Ö. "Harmonic differential quadrature-finite differences coupled approaches for geometrically nonlinear static and dynamic analysis of rectangular plates on elastic foundation", *J. of Sound and Vibration*, **294**, pp. 966-980 (2006).

5. Civalek, Ö. "Application of differential quadrature (DQ) and harmonic differential quadrature (HDQ) for buckling analysis of thin isotropic plates and elastic columns", *Engineering Structures*, **26**, pp. 171-186 (2004).

6. Civalek, Ö. "Nonlinear analysis of thin rectangular plates on Winkler-Pasternak elastic foundations by DSC-HDQ methods", *Applied Mathematical Modeling*, **31**, pp. 606-624 (2007).

7. Kwak, M.K. "Hydroelastic vibration of rectangular plates", *Transaction of the American Society of Mechanical Engineers, J. of Applied Mechanics*, **63**, pp. 110-115 (1996).

8. Haddara, M.R. and Cao, S. "A study of the dynamic response of submerged rectangular flat plates", *Marine Structures*, **9**, pp. 913-933 (1996).

9. Zhou, D. and Cheung, Y.K. "Vibration of vertical rectangular plate in contact with water on one side", *Earthquake Engineering and Structural Dynamics*, **29**, pp. 693-710 (2000).

10. Cheung, Y.K. and Zhou, D. "Coupled vibratory characteristics of a rectangular container bottom plate", *J. of Fluids and Structures*, **14**, pp. 339-357 (2000).

11. Chang, T.P. and Liu, M.-F. "On the natural frequency of a rectangular isotropic plate in contact with fluid", *J. of Sound and Vibration*, **236**, pp. 547-553 (2000).
12. Liang, C.C., Liao, C.C., Tai, Y.S. and Lai, W.H. "The free vibration analysis of submerged cantilever plates", *Ocean Engineering*, **28**, pp. 1225-1245 (2001).
13. Yadykin, Y., Tenetov, V. and Levin, D. "The added mass of a flexible plate oscillating in a fluid", *J. of Fluids and Structures*, **17**, pp. 115-123 (2003).
14. Jeong, K.-H. and Kim, J.-W. "Hydrostatic vibration analysis of two flexible rectangular plates partially coupled with liquid", *Nuclear Engineering and Technology*, **41**(3), pp. 335-345 (2009).
15. Jeong, K.-H., Lee, G.-M., Kim, T.-W. and Park, K.-B. "Free vibration of a rectangular plate partially in contact with a liquid at both sides", *The Korean Society for Noise and Vibration Engineering*, **18**(1), pp. 123-130 (2008) (In Korean).
16. Jeong, K.H., Yoo, G.H. and Lee, S.C. "Hydroelastic vibration of two identical rectangular plates", *J. of Sound and Vibration*, **272**, pp. 539-555 (2003).
17. Ergin, A. and Uğurlu, B. "Linear vibration analysis of cantilever plates partially submerged in fluid", *J. of Fluids and Structures*, **17**, pp. 927-939 (2003).
18. Zhou, D. and Liu, W. "Hydroelastic vibrations of flexible rectangular tanks partially filled with fluid", *Int. J. for Numerical Methods in Engineering*, **71**, pp. 149-174 (2007).
19. Uğurlu, B., Kutlu, A., Ergin, A. and Omurtag, M.H. "Dynamics of a rectangular plate resting on an elastic foundation and partially in contact with a quiescent fluid", *J. of Sound and Vibration*, **317**, pp. 308-328 (2008).
20. Amabili, M. "Eigenvalue problems for vibrating structures coupled with quiescent fluids with free surface", *J. of Sound and Vibration*, **231**(1), pp. 79-97 (2000).
21. Amabili, M. and Carra, S. "Thermal effects on geometrically nonlinear vibrations of rectangular plates with fixed edges", *J. of Sound and Vibration*, **321**, pp. 936-954 (2009).

APPENDIX

Effect of Hydrostatic Triangular Pressure

To account for the effect of hydrostatic triangular pressure, virtual work corresponding to hydrostatic triangular pressure is estimated by the following equations:

$$U_{h1} = \frac{1}{2}\rho_{F1} g \int_0^a \int_0^{b_1} w(b_1 - y)\,dy\,dx, \tag{A1}$$

$$U_{h2} = \frac{1}{2}\rho_{F2} g \int_0^a \int_0^{b_2} w(b_2 - y)\,dy\,dx, \tag{A2}$$

where U_{h1} and U_{h2} represent the virtual work associated with Tanks 1 and 2, respectively.

The virtual work due to hydrostatic triangular pressure can be taken into account for forced and nonlinear vibrations. In order to take into account the effects of hydrostatic triangular pressure on linear free vibration, a plate configuration due to hydrostatic triangular pressure has been developed. The plate configuration for thin plates, due to hydrostatic triangular pressure, can be approximated as:

$$w_{01} = \sum_{m=1}^{\infty}\sum_{n=1}^{\infty} A_{hp1}(m,n)\sin(m\pi x/a)\sin(n\pi y/b), \tag{A3}$$

where w_{01} is the plate configuration associated with Tank 1, due to the effect of hydrostatic triangular pressure, and A_{hp1} is the unknown constant coefficient. Applying bi-harmonic equation, $\nabla^4 w_{01} = -\rho_{F1} g(b_1 - y)$, coefficient A_{hp1} can be defined as:

$$\begin{aligned} &A_{hp1}(m,n)\pi^4((m/a)^2 \\ &\quad + (n/b)^2)^2 \sin(m\pi x/a)\sin(n\pi y/b) \\ &\quad = -\rho_{F1} g(b_1 - y). \end{aligned} \tag{A4}$$

From Equation A4, the associated Fourier coefficient, A_{hp1}, can be obtained:

$$A_{hp1}(m,n) = -\frac{\frac{1}{ab_1}\int_0^a\int_0^{b_1} \rho_{F1} g(b_1 - y)\sin(m\pi x/a)\sin(n\pi y/b)\,dy\,dx}{\pi^4((m/a)^2 + (n/b)^2)^2}. \tag{A5}$$

Similarly, the plate configuration associated with Tank 2 can be expressed as:

$$w_{02} = \sum_{m=1}^{\infty}\sum_{n=1}^{\infty} A_{hp2}(m,n)\sin(m\pi x/a)\sin(n\pi y/b), \tag{A6}$$

where:

$$A_{hp2}(m,n) = \frac{\frac{1}{ab_2}\int_0^a\int_0^{b_2} \rho_{F2} g(b_2 - y)\sin(m\pi x/a)\sin(n\pi y/b)\,dy\,dx}{\pi^4((m/a)^2 + (n/b)^2)^2}. \tag{A7}$$

The out-of-plane displacement representing the initial geometric deformations of the plate associated with zero initial hydrostatic triangular pressure tension is obtained as follows:

$$w_0 = w_{01} + w_{02}. \tag{A8}$$

The system has been then studied in the case of a plate contacting water on both sides. In this case, the contribution of the initial deformation of the plate, given by the hydrostatic pressure of the fluid, can be eliminated if the water level in both tanks is identical.

BIOGRAPHY

Korosh Khorshidi received a B.S. degree in Mechanical Engineering (Solid Mechanics) from the University of Mazandaran, Iran, in 2000. He obtained his M.S. and Ph.D. degrees in Mechanical Engineering (Solid Mechanics) from the Iran University of Science and Technology (IUST), Iran, in 2003 and 2008, respectively.

Dr. Khorshidi is currently the Assistant professor of Mechanical Engineering at Arak University, where since November 2009, he has been the head of Mechanical Engineering. His research interests include: Linear and Nonlinear Vibration, Sound Radiation and Impact of the Plate, Plate in Contact with Fluid, and Composite Plate. Dr. Khorshidi's research efforts have been published in several conferences and journals at national and international levels.